Anal. Chem. **2004,** *76,* 1213−1221

Accelerated Articles

Radiolytic Modification of Acidic Amino Acid Residues in Peptides: Probes for Examining Protein−Protein Interactions

Guozhong Xu[†,‡] and Mark R. Chance*[,†,‡,§]

Departments of Physiology & Biophysics and Biochemistry, and Center for Synchrotron Biosciences, Albert Einstein College of Medicine, 1300 Morris Park Avenue, Bronx, New York 10461-1602

Hydroxyl radical-mediated footprinting coupled with mass spectroscopic analysis is a new technique for mapping protein surfaces, identifying structural changes modulated by protein−ligand binding, and mapping protein−ligand interfaces in solution. In this study, we examine the radiolytic oxidation of aspartic and glutamic acid residues to probe their potential use as structural probes in footprinting experiments. Model peptides containing Asp or Glu were irradiated using white light from a synchrotron X-ray source or a cesium-137 γ-ray source. The radiolysis products were characterized by electrospray mass spectrometry including tandem mass spectrometry. Both Asp and Glu are susceptible to radiolytic oxidization by γ-rays or synchrotron X-rays. Radiolysis results primarily in the oxidative decarboxylation of the side chain carboxyl group and formation of an aldehyde group at the carbon next to the original carboxyl group, giving rise to a characteristic product with a −30 Da mass change. A similar oxidative decarboxylation also takes place for amino acids with C-terminal carboxyl groups. The methylene groups in the Asp and Glu side chains also undergo oxygen addition forming ketone or alcohol groups with mass changes of +14 and +16 Da, respectively. Characterizing the oxidation reactions of these two acidic residues extends the number of useful side chain probes for hydroxyl radical-mediated protein footprinting from 10 (Cys, Met, Trp, Tyr, Phe, Arg, Leu, Pro, His, Lys) to 12 amino acid residues, thus enhancing our ability to map protein surface structure and in combination with previously identified basic amino acid probes can be used to examine molecular details of protein−protein interactions that are driven by electrostatics.

Oxidative modification of protein side chains coupled with mass spectrometry analysis is a new technique for mapping protein surfaces and protein−ligand interactions.[1−14] The technique utilizes highly reactive hydroxyl radicals generated by radiolysis of water or Fenton's reagent to probe the detailed structure of proteins and their complexes,[1−4,9−14] extending the hydroxyl

* To whom correspondence should be addressed: (tel.) (718) 430 4136; (fax) (718) 430 8587; (e-mail) mrc@aecom.yu.edu.

† Department of Physiology & Biophysics.

‡ Department of Biochemistry.

§ Center for Synchrotron Biosciences.

(1) Chance, M. R. *Biochem. Biophys. Res. Commun.* **2001**, *287* (3), 614−21.
(2) Guan, J. Q.; Vorobiev, S.; Almo, S. C.; Chance, M. R. *Biochemistry* **2002**, *41* (18), 5765−75.
(3) Kiselar, J. G.; Maleknia, S. D.; Sullivan, M.; Downard, K. M.; Chance, M. R. *Int. J. Radiat. Biol.* **2002**, *78* (2), 101−14.
(4) Rashidzadeh, H.; Khrapunov, S.; Chance, M. R.; Brenowitz, M. *Biochemistry* **2003**, *42* (13), 3655−65.
(5) Wong, J. W.; Maleknia, S. D.; Downard, K. M. *Anal. Chem.* **2003**, *75* (7), 1557−63.
(6) Goldsmith, S. C.; Guan, J. Q.; Almo, S.; Chance, M. *J. Biomol. Struct. Dyn.* **2001**, *19* (3), 405−18.
(7) Sharp, J. S., Becker, J. M.; Hettich, R. L. *Anal. Biochem.* **2003**, *313* (2), 216−25.
(8) Maleknia, S. D.; Ralston, C. Y.; Brenowitz, M. D.; Downard, K. M.; Chance, M. *Anal. Biochem.* **2001**, *289* (2), 103−15.
(9) Liu, R.; Guan, J.-Q.; Zak, O.; Aisen, P.; Chance, M. R. *Biochemistry* **2003**, *75* (24), 6995−7007.
(10) Guan, J. G.; Almo, S. C.; Reisler, E.; Chance, M. R. *Biochemistry* **2003**, *42*, 11992−2000.
(11) Guan, J. Q.; Chance, M. R. Footprinting Methods to Examine the Structure and Dynamics of Proteins. In *Encyclopedia of Molecular Cell Biology and Molecular Medicine*; Meyers, R. A., Ed.; Wiley-VCH: Weinheim, Germany, in press.
(12) Guan, J. Q.; Almo, S.; Chance, M. R. *Acc. Chem. Res.*, published online Jan. 23, http://dx.doi.org/10.1021/ar0302235.
(13) Kiselar, J. G.; Almo, S. C.; Reisler, E.; Chance, M. R. *Mol. Cell. Proteomics* **2003**, *2*, 1120−32.
(14) Kiselar, J. G.; Janmey, P. A.; Almo, S. C.; Chance, M. R. *Proc. Natl. Acad. Sci. U.S.A.* **2003**, *100* (7), 3942−7.

10.1021/ac035422g CCC: $27.50 © 2004 American Chemical Society
Published on Web 02/03/2004

radical approaches originally applied to the study of nucleic acids.[15−19] Irradiation of aqueous solutions of biological macromolecules with X-rays[8,16,20,21] or γ-rays[17,19,22] results in hydroxyl radical-mediated oxidation of solvent-accessible and reactive moieties. Oxidized protein samples are typically analyzed by proteolysis and mass spectrometry coupled to high-performance liquid chromatography,[2,3,8,12] while the nucleic acids are analyzed by gel electrophoresis coupled with digital imaging analysis.[15,18,23] These footprinting approaches are quite powerful for revealing the structural details of macromolecular interactions.

Radiolytic footprinting of proteins depends on radiolytic modification of solvent-accessible and reactive amino acid side chains. Our previous studies indicated that the side chains of eight reactive amino acid residues, including Cys, Met, Phe, Tyr, Trp, Leu, Pro, and His, are convenient probes for mapping protein structure.[2,3,24] Radical-induced oxidation of peptides containing these residues generally leads to modified peptides with mass additions of +16 or +14 Da as a result of alcohol and ketone formation with the exception of His,[22,25,26] for which ring opening may result in the formation of products with mass changes of −22 or −23 Da (as a consequence of conversion of the His side chain to Asp or Asn) as well as −10 and +5 Da.[22] Recently, we have demonstrated that basic amino acid residues, especially arginine, are quite susceptible to oxidation and are useful probes for hydroxyl radical-mediated footprinting of proteins.[22] The oxidation of arginine is of particular interest as it gives rise to a characteristic product with a −43 Da mass change as result of oxidative elimination of the guanidino group.

The value of an amino acid residue as a probe of macromolecular interactions relies on its reactivity, its frequency of being on the surface, and its tendency to mediate protein−protein or protein−nucleic acid complex formation.[22] Systematic statistical analysis of residue frequencies and paring preferences at protein−protein interfaces has received considerate attention in recent years.[27−31] Protein−protein interfaces are generally rich in hydrophobic residues, and hydrophobic interactions contribute significantly to the binding energy. However, protein interfaces are generally less hydrophobic than protein cores; thus, the hydrophobic effect is considered to be less important to protein−protein interaction than it is to protein folding.[27] Charged amino acid residues are frequently found on the protein surface and are frequently buried in protein interfaces, particularly in the case of nonobligatory protein assemblies.[27,29,32] Hydrogen bonds and salt bridges at the interfaces contribute significantly to the stability of such protein−protein complexes;[33,34] in addition, they confer specificity for the interactions.[35] Because of the orientational requirements and the potential for long-range effects, electrostatic interactions are thought to mediate rapid binding kinetics in protein−protein associations.[36,37] The intermolecular ion pair network formed by the side chains of acidic and basic amino acid residues also plays a central role in the stability and functionality of thermophilic proteins.[38,39] Therefore, the development of charged amino acid residues as structural probes for footprinting has great value for analyzing protein structure and protein−protein interactions. In this work, we focus on examining the radiolytic oxidation of Asp and Glu to explore their suitability as structural probes for the dual purposes of developing probes to identify buried charge−charge interactions in protein complex interfaces and to expand the sequence coverage of protein footprinting techniques.

EXPERIMENTAL PROCEDURES

Materials. Peptides Asp-Asp-Asp-Asp (DDDD), Asp-Ser-Asp-Pro-Arg (DSDPR), Asp-Arg-Gly-Asp-Ser (DRGDS), *N*-acetyl-Asp-Arg-Gly-Asp-Ser (Ac-DRGDS), H-Glu-OH (glutamic acid), H-Glu-NH_2 (glutamic acid amide), H-Gln-OH (glutamine), H-Gln-NH_2 (glutamine amide), Ala-Asp-Ser-Asp-Gly-Lys (ADSDGK), Lys-Gln-Ala-Gly-Asp-Val (KQAGDV), Glu-Glu-Glu (EEE), Tyr-Pro-Phe-Val-Glu-Pro-Ile (YPFVEPI), Lys-Glu-Glu-Ala-Glu (KEEAE), Val-Glu-Ser-Ser-Lys (VESSK), Arg-Arg-Glu-Glu-Glu-Thr-Glu-Glu-Glu (RREEETEEE), and *N*-acetyl-Asp-OH were purchased from Bachem California Inc. (Torrance, CA). Peptide *N*-methyl-Glu-Glu-Glu-Pro-Ala-Ala-Arg-NH_2, with monomethylation at the N-terminus and amide modification at the C-terminus (CH_3-EEEPAAR-NH_2), was synthezed by Alpha Diagnostic (San Antonia, TX). All peptides had a purity at least of 95% and were used without further purification. B & J Brand high-purity acetonitrile was purchased from Honeywell International Inc. (Muskegon, MI). Solutions of peptides at a concentration of 20−40 μM were prepared in Nanopure water using a Millipore Ultrapure water system.

Exposure of Peptides to Radiation. The peptide solutions were exposed to either synchrotron X-rays at the X-28C beamline of NSLS at Brookhaven National Laboratory or a cesium-137 γ-ray source (1380 rads/min) at the Albert Einstein College of Medicine.

(15) Brenowitz, M.; Chance, M. R.; Dhavan, G.; Takamoto, K. *Curr. Opin. Struct. Biol.* **2002**, *12* (5), 648−53.
(16) Ralston, C. Y., et al., *Methods Enzymol.* **2000**, *317* 353−68.
(17) Tullius, T. D.; Dombroski, B. A.; Churchill, M. E.; Kam, L. *Methods Enzymol.* **1987**, *155* 537−58.
(18) Takamoto, K.; Chance, M. Footprinting Methods to Examine the Structure and Dynamics of Nucleic Acids. In *Encyclopedia of Molecular Cell Biology and Molecular Medicine*, 2nd ed.; Meyers, R. A., Ed.; Wiley Inc.: New York, 2003.
(19) Franchet-Beuzit, J.; Spotheim-Maurizot, M.; Sabattier, R.; Blazy-Baudras, B.; Charlier, M. *Biochemistry* **1993**, *32* (8), 2104−10.
(20) Chance, M. R.; Sclavi, B.; Woodson, S. A.; Brenowitz, M. *Structure* **1997**, *5* (7), 865−9.
(21) Sclavi, B.; Sullivan, M.; Chance, M. R.; Brenowitz, M.; Woodson, S. A. *Science* **1998**, *279*, 1940−3.
(22) Xu, G.; Takamoto, K.; Chance, M. R. *Anal. Chem.* **2003**, *75* (24), 6995−7007.
(23) Brenowitz, M.; Senear, D. F.; Shea, M. A.; Ackers, G. K. *Proc. Natl. Acad. Sci. U.S.A.* **1986**, *83*, 8462−6.
(24) Maleknia, S. D.; Brenowitz, M.; Chance, M. R. *Anal. Chem.* **1999**, *71* (18), 3965−73.
(25) Garrison, W. M., *Chem. Rev.* **1987**, *87* 381−98.
(26) Stadtman, E. R., *Methods Enzymol.* **1995**, *258*, 379−93.
(27) Tsai, C. J.; Lin, S. L.; Wolfson, H. J.; Nussinov, R. *Protein Sci.* **1997**, *6* (1), 53−64.
(28) Glaser, F.; Steinberg, D. M.; Vakser, I. A.; Ben-Tal, N. *Proteins* **2001**, *43* (2), 89−102.
(29) Ofran, Y.; Rost, B. *J. Mol. Biol.* **2003**, *325* (2), 377−87.
(30) Musafia, B.; Buchner, V.; Arad, D. *J. Mol. Biol.* **1995**, *254* (4), 761−70.
(31) Jones, S.; Thornton, J. M. *Proc. Natl. Acad. Sci. U.S.A.* **1996**, *93* (1), 13−20.
(32) Davis, S. J.; Davies, E. A.; Tucknott, M. G.; Jones, E. Y.; van der Merwe, P. A. *Proc. Natl. Acad. Sci. U.S.A.* **1998**, *95* (10), 5490−4.
(33) Xu, D.; Lin, S. L.; Nussinov, R. *J. Mol. Biol.* **1997**, *265* (1), 68−84.
(34) Lee, L. P.; Tidor, B. *Nat. Struct. Biol.* **2001**, *8* (1), 73−6.
(35) O'Shea, E. K.; Rutkowski, R.; Kim, P. S. *Cell* **1992**, *68* (4), 699−708.
(36) Schreiber, G.; Fersht, A. R. *Nat. Struct. Biol.* **1996**, *3* (5), 427−31.
(37) Frisch, C.; Fersht, A. R.; Schreiber, G. *J. Mol. Biol.* **2001**, *308* (1), 69−77.
(38) Sarin, J.; Raghava, G. P.; Chakraborti, P. K. *Protein Sci.* **2003**, *12* (9), 2118−20.
(39) Matsumiya, S.; Ishino, S.; Ishino, Y.; Morikawa, K. *Protein Sci.* **2003**, *12* (4), 823−31.

Radiolysis using synchrotron X-rays and low-flux γ-rays induces similar modifications of biological macromolecules,[22] except the time scales of significant modifications are milliseconds for synchrotron X-rays and minutes for low-flux γ-rays. Because some of the low-MW peptides examined in this study are oxidized too rapidly by the high-flux synchrotron source to give accurate dose response data (the shutter's lower limit is 7 ms), the dose response data were derived using the cesium-137 γ-ray source. Ten microliters of 40 μM peptide solutions in 0.2-mL Eppendorf tubes were exposed at synchrotron X-ray beamline X-28C using the stand and shutter. These samples were irradiated for 10−30 ms at beam currents ranging from 180 to 290 mA in accordance with our established protocols.[2,3] For samples exposed to the cesium-137 source, 30 μL of a 20 μM peptide solution in a 1.5-mL Eppendorf tube was exposed for 0.5−30 min. The exposure time was also controlled electronically.[22] After exposure to radiation, all peptide samples were stored at −20 °C before analysis.

Mass Spectrometric Analysis of Peptides. The irradiated peptides were analyzed directly by electrospray mass spectrometry without chromatographic separation. The peptide concentrations were adjusted to 10 μM with acetonitrile and were infused directly into the ESI-MS at a flow rate of 3 μL/min. Mass spectra were acquired on a Finnigan LCQ quadrupole ion trap mass spectrometer (Finnigan Corp., San Jose, CA) with a mass accuracy of ±0.2 amu and unit resolution. The needle voltage was set at 4.5 kV. The instrument was tuned using the known masses of the unmodified peptides. All spectra were recorded in the profile mode as indicated in the results. To determine the sites of amino acid oxidation, the collision-induced dissociation (CID) MS/MS spectra and MS/MS/MS spectra were acquired for selected ions.

Detection of Aldehyde Products by Color Reaction. The Purpald color reaction was performed according to a procedure slightly modified from that in the literature.[40] Purpald was dissolved in 1.0 M NaOH to a concentration of 0.75%. Twenty microliters of 2.0 mM H-Glu-NH_2 was exposed to γ-rays for 3 h and mixed with 60 μL of Pupald solution in a 0.2-mL Eppendorf tube and then 5 μL of 30% H_2O_2 was added to the mixture. The sample was briefly vortexed and allowed to stand for a few minutes, after which the color was noted.

Data Processing. The data are processed according to the procedure described previously.[22] Limited modification of a peptide in the typical protein footprinting condition may affect the ionization efficiency to some extent but not significantly, except in the case of Arg, whose oxidative loss of the guanidino group greatly reduces ionization efficiency in positive electrospray mode. Therefore, the oxidation products are measured according to their peak intensity of mass spectral signals; e.g., no correction is made for potential ionization efficiency differences between unoxidized and oxidized products. The amount of unoxidized peptide (fraction unmodified M) is calculated by the ratio of peak intensity of unoxidized peptide to the sum of peak intensities of unoxidized peptide and all oxidation products, whereas the amount of a specific oxidation product (fraction modified P_i) is measured by the ratio of its peak intensity to the sum of peak intensities of unoxidized peptide and all oxidation products. The kinetics of radiolytic modification is studied by the dose response, i.e., the decay of unoxidized peptide or the accumulation of oxidation products as a function of exposure time. The processes follow pseudo-first-order reaction kinetics.[2,3,22] The apparent rate constant k_u of decay of the unoxidized peptide is obtained by nonlinear fitting of fraction unmodified (M) and its corresponding exposure time (t) into eq 1, while the rate constant k_i for production of the ith oxidation product is obtained by fitting the fraction modified P_i and exposure time t into eq 2.

Scheme 1. Proposed Mechanism for Oxidative Decarboxylation of C-Terminal Amino Acid[a]

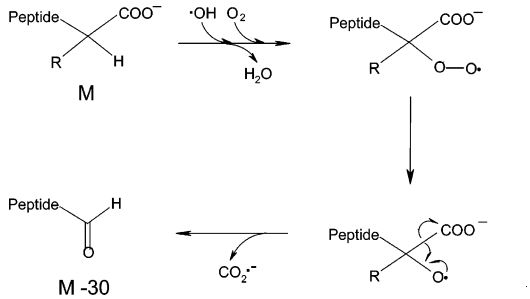

[a] R = side chain.

$$M = e^{-k_u t} \quad (1)$$

$$P_i = (k_i/k_u)(1 - e^{-k_u t}) \quad (2)$$

RESULTS AND DISCUSSION

Decarboxylation of the C-Terminal Carboxyl Group. In our previous studies on the radiolysis of the peptide Ala-Arg-Arg-Ala, we found an oxidation product exhibiting a 30 Da mass reduction compared to the original peptide.[22] The MS/MS spectrum of the −30 Da species indicated the 30 Da reduction arose from the C-terminal residue. Formation of the −30 Da product is common in radiolysis of peptides and proteins and is characteristically observed for peptides with unmodified C-terminal carboxyl groups in this work. If the C-terminal carboxyl is modified by amidation (see below), the −30 Da oxidation product is not observed.

It has been previously reported that generation of protein and peptide alkoxyl radicals can give rise to C-terminal decarboxylation.[41] Irradiation of *N*-acetyl amino acids and dipeptides produces hydroperoxides at the α-carbon position of the C-terminal residue. Decomposition of the α-carbon hydroperoxide by incubation of the irradiated samples with Fe(II)-EDTA resulted in C-terminal decarboxylation via a pseudo-Fenton reaction with release of radical $CO_2^{\bullet-}$, which was trapped and detected by EPR spectroscopy. A mechanism of decarboxylation as outlined in Scheme 1 was proposed to explain the release of radical $CO_2^{\bullet-}$, and the α-carbon alkoxyl radical was thought to be the key intermediate in the process. The corresponding amides were proposed to undergo deamidation with release of $^{\bullet}CONH_2$. The proposed oxidation mechanism generates a new carbonyl group at the original α-carbon.[41] Although we have no evidence to directly support this oxidation mechanism, we do observe products having a −30 Da mass change consistent with it. However, the deamidation of C-terminal amide, which should generate a −29 Da product, is not found in our studies.

(40) Dickinson, R. G.; Jacobsen, N. W. *Chem. Commun.* **1970**, 1719−20.

(41) Davies, M. J. *Arch. Biochem. Biophys.* **1996**, *336* (1), 163−72.

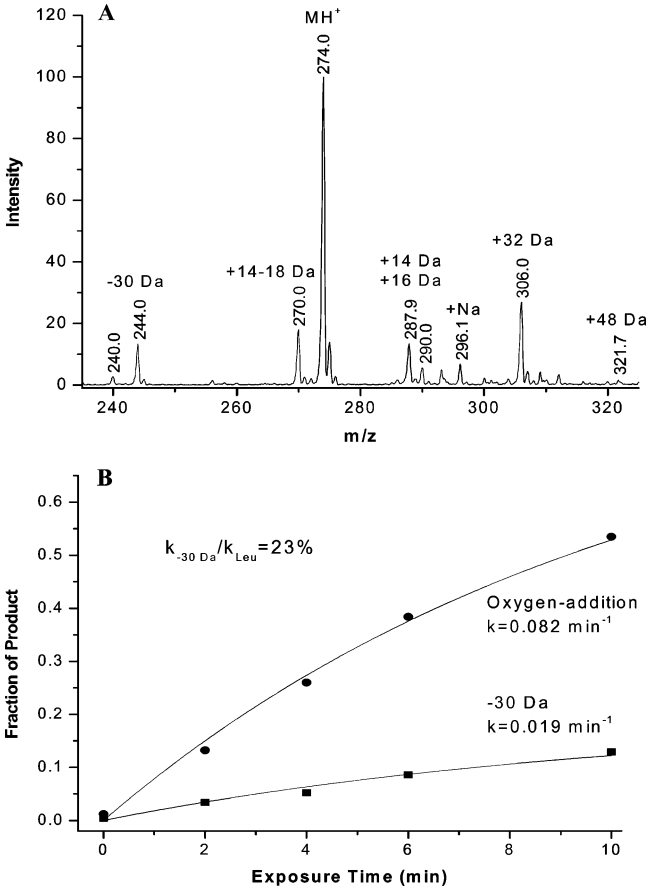

Figure 1. (A) ESI-MS spectrum of 20 μM peptide ALA exposed to γ-rays for 6 min. The exposed samples were diluted to 10 μM using acetonitrile and analyzed by ESI-MS without chromatographic separation. (B) Dose response curves of oxygen-addition products (+14 and +16 Da) and decarboxylation product (−30 Da). The solid lines are fits to the data as described in the Experimental Procedures section.

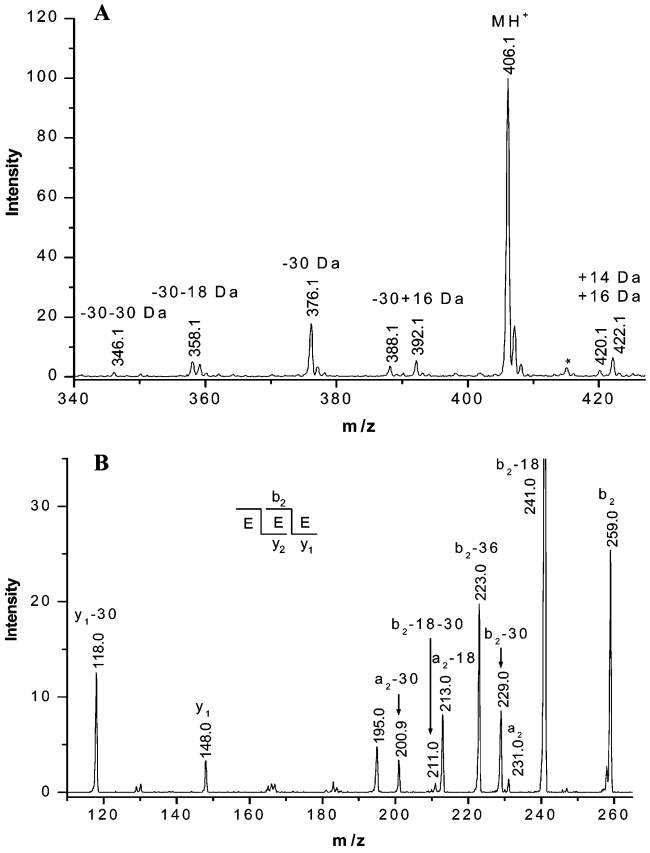

Figure 2. (A) ESI-MS spectrum of 20 μM peptide EEE exposed to γ-rays for 6 min. $*$ is an impurity. (B) MS/MS spectrum of $(MH - 30)^+$ ion at *m*/*z* 376.1.

The kinetics of C-terminal decarboxylation is analyzed by dose response experiments on the peptides Ala-Leu-Ala (ALA) and Gly-Leu-Gly (GLG). Figure 1A shows a positive ESI-MS spectrum of ALA irradiated by γ-rays for 6 min. The peak at *m*/*z* 274.0 is the unmodified peptide. The peaks at *m*/*z* 287.9, 290.0, and 306.0 are the +14 Da, +16 Da, and +16 × 2 oxygen-addition products, respectively. The signal at *m*/*z* 244.0 is the characteristic −30 Da product. In the MS/MS spectrum of the −30 Da species at *m*/*z* 244.0 (not shown), only two fragments, b_2 and a_2 ions, were present; no $b_2 - 30$ or other fragments were observed. This indicates that the −30 Da oxidation arises from the C-terminal Ala. In the MS/MS spectrum of the +14 Da species at *m*/*z* 287.9 (not shown), only fragment ions $b_2 + 14$ and $a_2 + 14$ were observed, and no a_2, b_2, or y_2 ions were found. The MS/MS spectra of the +16 Da species at *m*/*z* 290.0 and the +32 Da species at *m*/*z* 306.0 (not shown) are similar to that of *m*/*z* 287.9. The data indicate that the +14 and +16 Da oxygen-addition products do not arise from the C-terminal Ala. The rate constant for reaction of hydroxyl radical with Leu is 1.7×10^9 and 7.7×10^7 M^{-1} s^{-1} for Ala,[42] suggesting that hydroxyl reaction with Leu is 22 times faster than with Ala under comparable conditions. Moreover, the N-terminal alanine is further deactivated by proximity to the positively charged protonated amine. Thus, it is logical that the oxygen-addition products should arise primarily from the oxidation of the Leu side chain. The rates of formation of the −30 Da product and the oxygen-addition products represent the rates of C-terminal oxidative decarboxylation and oxidation of the Leu residue. The dose response for the formation of −30 Da and all oxygen-addition products in radiolysis of ALA is presented in Figure 1B. The rate constant is 0.082 min^{-1} for formation of oxygen-addition products and 0.019 min^{-1} for formation of the −30 Da products. The data indicated that rate of C-terminal decarboxylation is 23% compared to that of Leu oxidation. A similar dose response for peptide GLG was also performed (not shown), and the rate of C-terminal decarboxylation is 46% compared to that of oxidation of Leu, 2-fold of that seen for ALA. This is reasonable since Gly has two α-hydrogen atoms while Ala has only one.

Decarboxylation of Glutamic Acid Residues. *EEE.* To simplify the examination of side chain oxidations, a simple peptide Glu-Glu-Glu (EEE) was selected to investigate the radiolytic modification of glutamic acid. Peptide EEE, at a concentration of 20 μM, was exposed to γ-rays for 6 min and the positive ESI-MS spectrum is shown in Figure 2A. The unmodified peptide appears at *m*/*z* 406.1, while the dominant product appears at *m*/*z* 376.1, 30 mass units lower. The commonly seen +14 and +16 Da oxidation products are found at *m*/*z* 420.1 and 422.1. These oxygen-additions occur at any methene carbon of the side chains

(42) Buxton, G. V.; Greenstock, C. L.; Helman, W. P.; Ross, A. B. *J. Phys. Chem. Ref. Data* **1988**, *17*, 513−886.

of the three Glu residues. Multiple oxidation products with −30 × 2 and −30 + 16 Da are also present at *m*/*z* 346.1 and 392.1.

Tandem mass spectra were acquired to determine the modification sites on the peptide for each oxidation product using CID. The peptide fragments are named according to the Biemann nomenclature.[43] Cleavage of the peptide chain may occur at the C_α−C, C−N, or N−C_α bonds within the peptide and yields fragment ions a_n, b_n, and c_n, with charge(s) retained on the N-terminal side of the peptide, and x_n, y_n, and z_n, with charge(s) retained on the C-terminal side, with the *n* value denoting the size of the fragments in amino acids.The MS/MS spectrum of *m*/*z* 376.1 (−30 Da) is shown in Figure 2B. The peaks at *m*/*z* 148.0 and 118.0 correspond to y_1 and y_1 − 30 ions. Observation of the y_1 − 30 ion implies oxidative decarboxylation of C-terminal Glu, while appearance of the y_1 ion indicates the N-terminal and middle Glu residues also give rise to −30 Da products. This conclusion is further supported by observation of a b_2 ion at *m*/*z* 259.0 and a b_2 − 30 ion at *m*/*z* 229.0. The data indicates that the −30 Da mass loss can be located at any Glu residue of the peptide. There are a few fragments of medium intensity due to the loss of 1, 2, or 3 H_2O molecules from the parent ion; there are three carboxyl groups that remain in the −30 Da selected ions that can lose 1, 2, or 3 waters. The intensity of the b_2 − 18 ion is ∼3.5-fold greater than the b_2 ion; this indicates that carboxyl groups easily lose a neutral water molecule. The relative intensity of b_2 and b_2 − 18 ions compared to those of b_2 − 30 related ions suggests the C-terminal Glu contributes to the formation of −30 Da products more than the N-terminal and middle Glu residues.

RREEETEEE. The second Glu-containing peptide that was examined is RREEETEEE. The peptide was exposed to synchrotron X-rays for 10 ms, and the positive ESI-MS spectrum is shown in Figure 3A. The inset contains the amplified singly charged signals. The peaks at *m*/*z* 603.8 and 1206.5 correspond to the doubly and singly charged unmodified peptides. The peaks at *m*/*z* 610.7 and 1220.4 are the doubly and singly charged ions of +14 Da products, while the signals at *m*/*z* 611.7 and 1222.4 correspond to the +16 Da products. Oxidative decarboxylation gives rise to characteristic −30 Da oxidation products, which appear at *m*/*z* 588.8 as doubly charged and 1176.5 as singly charged signals. The weak signals corresponding to further loss of water (−18 Da) or an additional −30 Da as well as oxygen addition to the −30 Da product observed as doubly charged signals at *m*/*z* 579.8 (−30 − 18 Da), 573.8 (−30 − 30 Da), 595.8 (−30 + 14 Da), and 596.7 (−30 + 16 Da), and as singly charged signals at *m*/*z* 1190.4 (−30 + 14 Da), and 1192.4 (−30 + 16 Da). The oxidation of Arg also gives rise to the characteristic products at *m*/*z* 1163.5 (−43 Da), 1145.5 (−43 − 18 Da), 1133.4 (−43 − 30 Da), and 1115.4 (−43 − 30 − 18 Da). The −43 Da related signals are weak because of reduced ionization efficiency as a result of loss of the guanidine in Arg.

The MS/MS spectrum of the doubly charged −30 Da signal at *m*/*z* 588.8 is shown in Figure 3B. There are no y-type fragment ions present in the MS/MS spectrum because the two charges of the parent ion are fixed at the two Arg residues at the N-terminus. The signal at *m*/*z* 313.1 is the unmodified b_2 fragment, while no b_2 − 30 is found. The presence of b_2 and absence of b_2 − 30 indicate the two Arg residues do not contribute to the −30 Da product. The peak at *m*/*z* 441.8 is the b_3 ion, while the signal at *m*/*z* 412.1 is the b_3 − 30 ion. The absence of b_2 − 30 and presence of b_3 − 30 indicate a 30 Da mass loss at the Glu next to the Arg, while the presence of b_3 implies a 30 Da mass loss from the peptide segment EETEEE. The peaks at 286.1 and 271.2 are doubly charged b_4^{2+} and $(b_4 - 30)^{2+}$ ions, respectively. The signals at *m*/*z* 350.6 and 335.7 are doubly charged b_5^{2+} and $(b_5 - 30)^{2+}$ ions, respectively. The peaks at *m*/*z* 401.1 and 385.9 are b_6^{2+} and $(b_6 - 30)^{2+}$ ions, respectively. The peaks at *m*/*z* 465.7 and 450.7 are b_7^{2+} and $(b_7 - 30)^{2+}$ ions, respectively. The signals at *m*/*z* 530.2 and 515.2 are b_8^{2+} and $(b_8 - 30)^{2+}$ ions, respectively. These data indicate that the −30 Da mass loss arises from both C-terminal and internal glutamic acid residues.

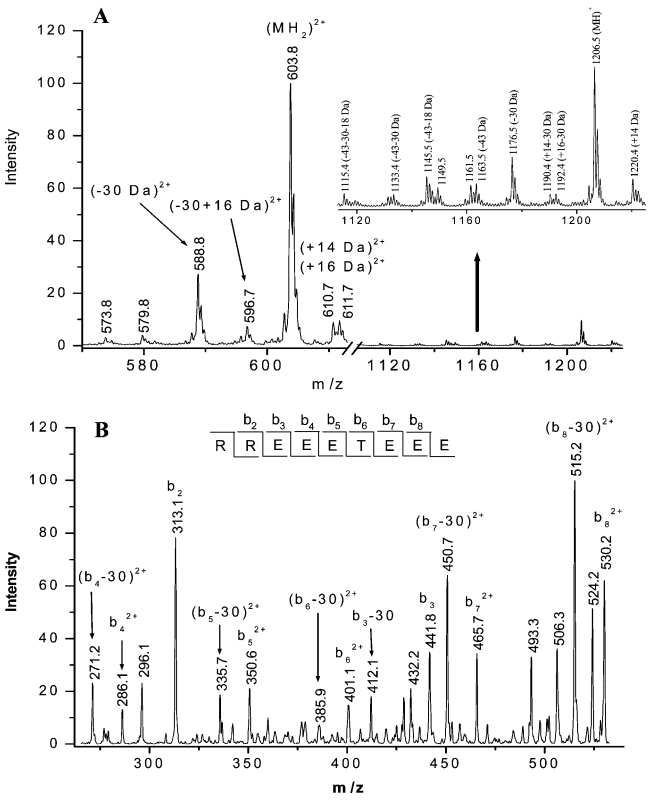

Figure 3. (A) ESI-MS spectrum of 40 μM peptide RREEETEEE exposed to synchrotron X-rays for 10 ms; the inset is the amplification of singly charged signals. (B) MS/MS spectrum of $(MH_2 - 30)^{2+}$ ion at *m*/*z* 588.8.

CH_3-EEEPAAR-NH_2. To eliminate the complication due to decarboxylation of the C-terminal carboxyl group, a third peptide CH_3-EEEPAAR-NH_2 with a C-terminal amide was investigated. The peptide at a concentration of 20 μM was exposed to γ-rays for 6 min, and the positive ESI-MS spectrum is shown in Figure 4A. The peak at *m*/*z* 814.3 corresponds to the unmodified peptide. The signal at *m*/*z* 784.3, which is 30 Da lower than the original peptide, results from the oxidative decarboxylation of Glu residues. The oxidation of Arg gives rise to the characteristic −43 Da product at *m*/*z* 771.1, which is weak because of significantly reduced ionization efficiency as a result of destruction of the positively charged guanidino group.[22] The peaks at *m*/*z* 828.3 and 830.3 are +14 and +16 Da products, which are primarily produced by the oxidation of Pro and Arg as discussed previously.[22]

The site of the 30 Da mass loss is examined by tandem mass spectrometry. The MS/MS spectrum of *m*/*z* 784.3 (−30 Da) is

(43) Biemann, K. *Methods Enzymol.* **1990**, 886−7.

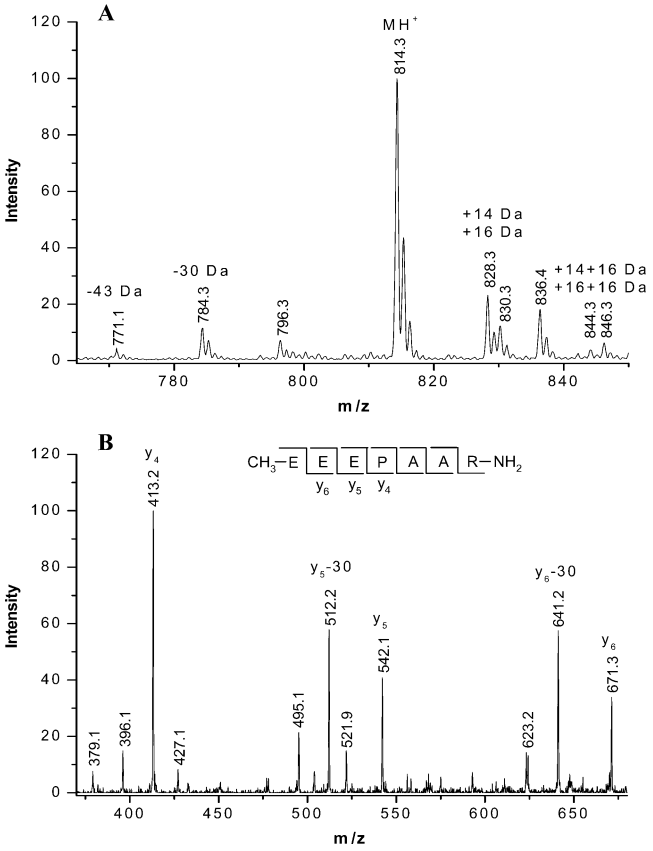

Figure 4. (A) ESI-MS spectrum of 20 μM peptide CH_3-EEEPAAR–NH_2 exposed to γ-rays for 6 min. (B) MS/MS spectrum of $(MH - 30)^+$ ion at *m*/*z* 784.3.

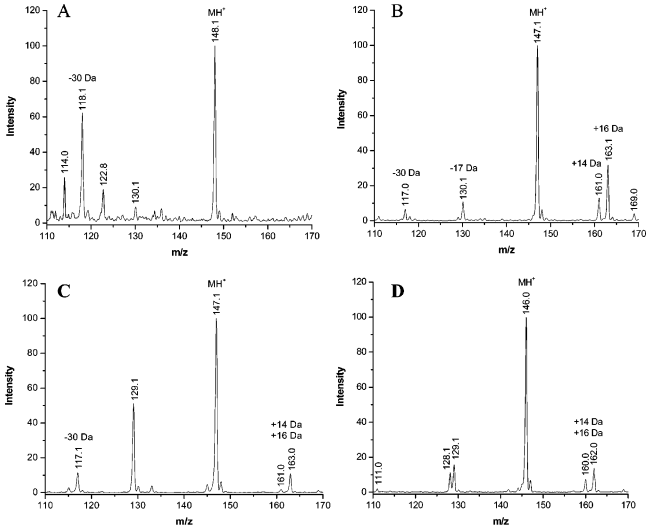

Figure 5. ESI-MS spectra of 20 μM glutamic acid and its derivatives irradiated by γ-rays: (A) Glu-OH, 16 min; (B) Gln-OH, 16 min; (C) Glu-NH_2, 12 min; and (D) Gln-NH_2, 10 min.

shown in Figure 4B. An intense y_4 ion is found at *m*/*z* 413.2. No $y_4 - 30$ ion is found. The presence of an intense y_4 ion and absence of the $y_4 - 30$ ion indicate the 30 Da mass loss is not located at PAAR but at EEE. The peaks at *m*/*z* 542.1 and 512.1 are y_5 and $y_5 - 30$ ions, respectively. The presence of $y_5 - 30$ and y_4 ions and the absence of $y_4 - 30$ ions suggest the loss of 30 Da mass from the Glu next to Pro, while the presence of y_5 implies the loss of 30 Da mass from the two Glu residues at the N-terminus. The peaks at *m*/*z* 671.3 and 641.2 correspond to y_6 and $y_6 - 30$ ions, respectively. The presence of a y_6 ion indicates the loss of 30 Da at the N-terminal Glu. In conclusion, the 30 Da mass loss is exclusively located at the three Glu residues and all the three Glu residues contributed to the −30 Da oxidation products. Other Glu-containing peptides were investigated including YPFVEPI, KEEAE, and VESSK. Radiolysis of these peptides in water all generated −30 Da products.

Glutamic Acid Derivatives. To conclusively confirm that the side chain carboxyl of Glu gives rise to −30 Da products, we examined the radiolytic oxidation of amino acids glutamic acid (Glu-OH) and glutamine (Gln-OH) and their amidated derivatives, Glu-NH_2 and Gln-NH_2. The positive ESI-MS spectrum of glutamic acid irradiated for 15 min is shown in Figure 5A. A very strong −30 Da signal is observed at *m*/*z* 118.1, and no signals corresponding to +14 or +16 Da products are found. The −30 Da products are contributed by decarboxylation of both side chain and C-terminal carboxyl groups. When the carboxyl group in either side chain or C-terminus is blocked by an amide as in the cases of Gln-OH (Figure 5B) and Glu-NH_2 (Figure 5C), a −30 Da product is still generated, but at a reduced amount, and +14 and +16 Da oxygen-addition products are increased. However, if both side chain and C-terminal carboxyl groups are blocked by amide as in the case of Gln-NH_2 (Figure 5D), no −30 Da species is produced. These data confirm the data from the peptides that both C-terminal and side chain carboxyl group can be oxidized to −30 Da products.

The oxidative decarboxylation presented in Scheme 1 generates an aldehyde group in the carbon in the side chain next to the original group. The presence of aldehyde products was confirmed by the Purpald color reaction. Even though Purpald reagent reacts with both aldehydes and ketones, only the aldehyde product is further oxidized to yield a purple-to-magenta aromatic heterocyclic product (6-mercapto-*s*-triazolo-[4,3-b]-*s*-tetrazines) on exposure to air or hydrogen peroxide. The color reaction was carried out on γ-ray exposed Glu-NH_2 as outlined in Experimental Procedures, and a pink color was formed. The color is weak because of small amount of aldehyde present in the sample.

Kinetics of Oxidative Decarboxylation of Glu. The kinetics of oxidative decarboxylation of Glu were investigated by comparison to oxidation of Phe and Pro, both of which are reactive and useful probes for protein footprinting. To simplify the study, the amino acid amides Glu-NH_2, Phe-NH_2, and Pro-NH_2 were used. A mixture containing 30 μM Glu-NH_2 and 10 μM Phe-NH_2 or 10 μM Pro-NH_2 was exposed to γ-rays for different lengths of time. A higher concentration of Glu-NH_2 was used because of its 3-fold lower ESI ionization efficiency compared to Phe-NH_2 and Pro-NH_2. The dose response curves for Glu-NH_2/Phe-NH_2 and Glu-NH_2/Pro-NH_2 are shown in Figure 6A and B, respectively. The data are processed and the rate constants were obtained by nonlinear fitting as described in Experimental Procedures. For the mixture of Glu-NH_2 and Phe-NH_2, a rate constant of 0.0064 min^{-1} was obtained for Glu-NH_2 and a rate constant of 0.1245 min^{-1} for Phe-NH_2. Thus, the rate of Glu-NH_2 oxidation is 5.1% that of Phe-NH_2. For the mixture of Glu-NH_2 and Pro-NH_2, a rate constant of 0.0114 min^{-1} was obtained for Glu-NH_2 and a rate constant of 0.0156 min^{-1} for Pro-NH_2; the rate of Glu-NH_2 oxidation is 73% that of Pro-NH_2.

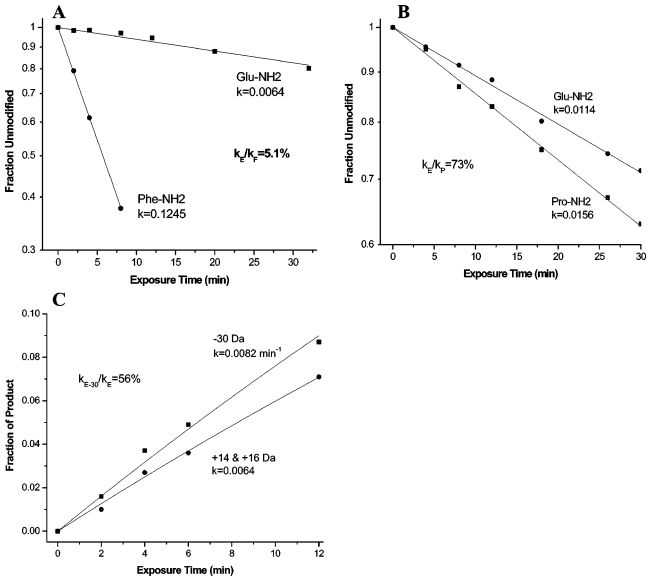

Figure 6. Dose response curves of (A) a mixture of 30 μM Glu-NH_2 and 10 μM Phe-NH_2; (B) a mixture of 30 μM Glu-NH_2 and 10 μM Pro-NH_2; (C) decarboxylation (−30 Da) and oxygen-addition (+14 & +16 Da) products of 20 μM Glu-NH_2 irradiated by γ-rays. The solid lines are fits to the data as described in Experimental Procedures.

The dose response analysis of Glu-NH_2 was also carried out at a concentration of 20 μM to compare the relative amounts of different oxidation products of Glu radiolysis. The dose response curves of decarboxylation (−30 Da) and oxygen-addition products (+14, +16 Da) are shown in Figure 6C. The rate constants are 0.0082 and 0.0064 min^{-1} for formation of the decarboxylation and oxygen-addition products; decarboxylation accounts for 56% of total oxidation products.

Mechanism of Oxidative Decarboxylation of Glu. There are few reports of radiolytic oxidation of acidic amino acid residues compared to the numerous reports of metal-catalyzed oxidation.[44] Like other amino acids with aliphatic hydrocarbon side chains, radiolytic oxidation of Glu in the presence of O_2 gives rise to alcohols (+16 Da), carbonyl (+14 Da), or hydroperoxide (+32 Da) in the side chain as a result of formation of an initial carbon-centered radical via hydrogen abstraction by hydroxyl radical and addition of O_2 to generate a peroxyl radical. In addition to the above reactions, γ-carbon-centered peroxyl radicals may also undergo a complicated reaction giving rise to an unsaturated product and oxalic acid via decomposition of side chain.[25,26] This unsaturated product will experience a 60 Da mass reduction compared to the original Glu residue (Scheme 2). However, the −60 Da product is not detected in our studies. Similar to the C-terminal decarboxylation discussed above (Scheme 1), a mechanism of oxidative decarboxylation for the Glu side chain was suggested by Davies.[45] In this study, glutamate and bovine serum albumen were exposed to γ-rays. After exposure, catalase was added to destroy the radiation-generated H_2O_2, and then the irradiated samples were incubated with Fe(II)-EDTA. During incubation, a negative radical $CO_2^{\bullet-}$ was generated, spin-trapped, and detected by EPR. A mechanism similar to that of decarboxylation of C-terminal carboxyl as shown in Scheme 1 was proposed to account for the formation of $CO_2^{\bullet-}$. The mechanism is reasonable to explain the −30 Da product of Glu generated by radiolysis. The possible oxidation products of Glu are outlined in Scheme 2.

Scheme 2. Proposed Oxidation Products of Glutamic Acid Residues[a]

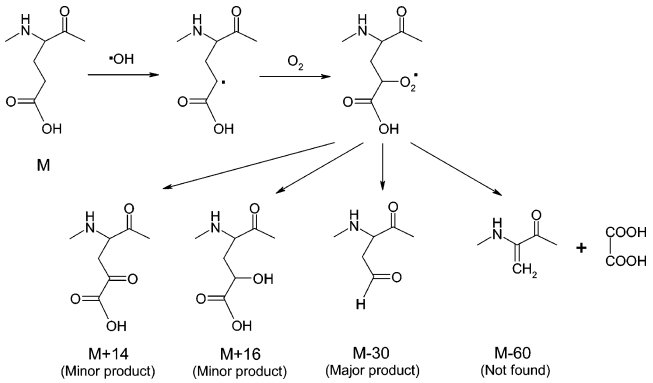

[a] The M − 60 Da product suggested in the literature is not seen.

The preferred formation of the −30 Da decarboxylation product can by explained by the selectivity of hydroxyl attack and the proximity of the side chain carboxyl group. In weak acidic or neutral pH conditions, the carboxyl group dissociates to give a negatively charged carboxylate group, which makes the neighboring carbon (γ-carbon) a preferred site for hydroxyl attack, as the resultant carbon-centered radical can be stabilized by the adjacent electron-rich carboxylate group through electron delocalization.

Decarboxylation of Aspartic Acid Residues. *DDDD*. A simple peptide, Asp-Asp-Asp-Asp (DDDD), was selected to investigate the radiolytic modification of aspartic acid residues. The peptide at a concentration of 40 μM was exposed to synchrotron X-rays for 10 ms, and the positive ESI-MS spectrum is shown in Figure 7A. The peak at m/z 479.0 corresponds to the molecular ion of the unmodified peptide. The peaks at m/z 461.0 and 501.1 are due to the loss of a water molecule and sodium adducts of the unmodified peptide, respectively. The second most intense signal at m/z of 449.0 Da is the major modified product, which is 30 Da lower than that of the unmodified peptide. The product at m/z 471.1 is the same as that at m/z 449.0, but with sodium attached to it. Other modification products include those with m/z 495.0 (+16), 465.0 (−30, +16), and 405.1 (−30, −44).

The MS/MS spectrum of ion m/z 449.0 (−30 Da) is presented in Figure 7B. The peaks at m/z 345.9 and 315.9 are unmodified b_3 and modified b_3 − 30 CID ions, while the peaks at m/z 327.9 and 298.0 are due to the loss of a water molecule from these two ions. Observation of the b_3 ion indicates a loss of 30 Da at the C-terminal Asp residue, while the presence of the b_3 − 30 ion indicates loss of 30 Da mass among the three N-terminal Asp residues. The peaks at m/z 230.9 and 203.0 are b_2 and a_2 ions, respectively. The peak at m/z 200.9 is the b_2 − 30 ion, which indicates a loss of 30 Da mass from either of the two N-terminal Asp residues. The signals at m/z 249.0 and 218.9 belong to y_2 and y_2 − 30 ions, indicating loss of 30 Da mass on both the former two and the last two Asp residues. Overall, oxidation of aspartic acid residues results in products with a 30 Da mass reduction.

(44) Davies, M. J.; Fu, S.; Wang, H.; Dean, R. T. *Free Radical Biol. Med.* **1999**, *27* (11−12), 1151−63.
(45) Davies, M. J.; Fu, S.; Dean, R. T. *Biochem. J.* **1995**, *305*, 643−9.

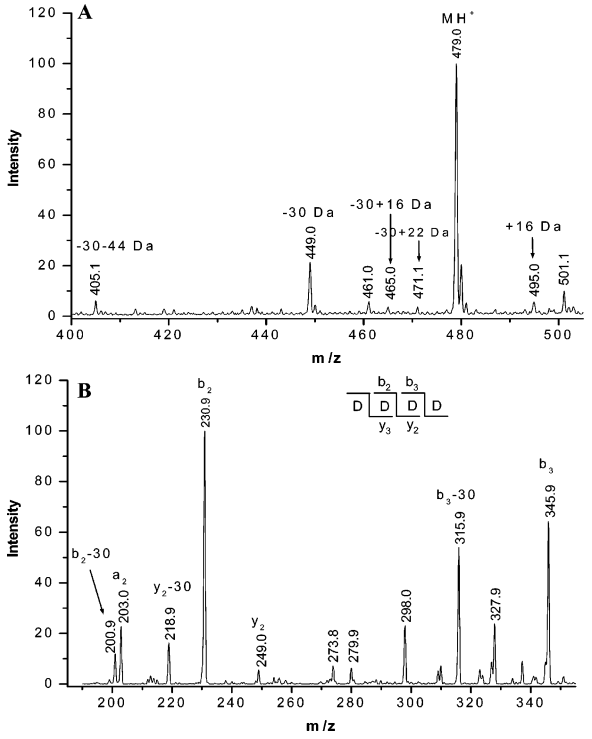

Figure 7. (A) ESI-MS spectrum of 40 μM peptide DDDD exposed to synchrotron for 10 ms. (B) MS/MS spectrum of $(MH - 30)^+$ ion at *m*/*z* 449.0.

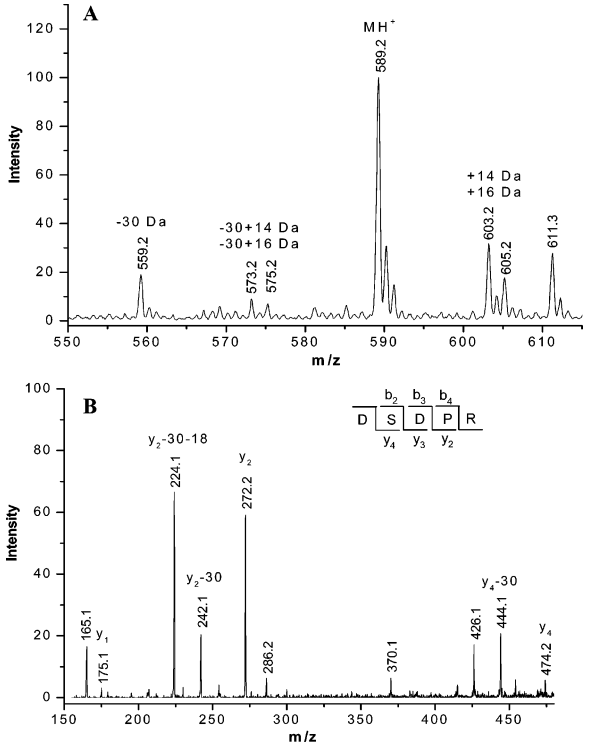

Figure 8. (A) ESI-MS spectrum of 20 μM peptide DSDPR exposed to γ-rays for 6 min. (B) MS/MS spectrum of $(MH - 30)^+$ ion at *m*/*z* 559.2.

The other modification products, including *m*/*z* 495.0, 465.0, and 405.1, were also identified by tandem mass spectra. The peak at *m*/*z* 495.0 is an oxidation product with 16 Da mass addition. The MS/MS spectrum (not shown) shows b_2, $b_2 + 16$, b_3, $b_3 + 16$, y_2, $y_2 + 16$, and $y_3 + 16$ ions, which indicate that both C-terminal and internal aspartic residues can be oxidized to a +16 Da product. The +16 Da oxidation product is commonly seen in radiolysis of many amino acid residues. The signal at *m*/*z* 465.0 is $-30 + 16$ Da relative to the original peptide and is a product resulting from oxidative decarboxylation (−30 Da) and oxygen addition (+16 Da). The peak at *m*/*z* 405.1 is an additional decarboxylation product from *m*/*z* 449.0 by loss of CO_2 (44 Da), which is common for compounds containing carboxyl group(s).

DSDPR. DSDPR was investigated for its radiolysis products. The peptide was chosen for its simplicity and known fragmentation between Asp and Pro residues to give a clear MS/MS spectrum. The peptide at 20 μM concentration was exposed to γ-rays for 6 min, and the positive ESI-MS spectrum is presented in Figure 8A. The peak at *m*/*z* 559.2 is 30 mass units lower, while the peaks at *m*/*z* 603.2 and 605.2 are 14 and 16 mass units higher than the original peptide at *m*/*z* 589.2. The +14 and +16 oxygen-addition products mostly result from the oxidation of Pro and Arg. The signals at *m*/*z* 573.2 and 575.2 are 30 Da below *m*/*z* 603.2 and 605.2 and apparently result from multiple oxidations. The peak at *m*/*z* 611.3, which is 22 Da above the unmodified peptide, corresponds to the sodium adduct of the unmodified peptide. The radiolysis of Arg residue produces a characteristic −43 Da product due to oxidative cleavage of the guanidino group. The expected −43 Da product at *m*/*z* 546.2 was not seen in the positive electrospray mass spectrum because of significantly reduced ionization efficiency as a result of loss of the charged guanidino group from Arg. However, the −43 Da product was clearly seen with high intensity at *m*/*z* 544.2 in a negative electrospray mass spectrum (not shown).

The MS/MS spectra of positive and negative ions of the oxidized product provided complementary information for determining the sites of oxidation and indicated that both the Asp residues and the C-terminus in DSDPR are responsible for the 30 Da mass reduction. The positive MS/MS spectrum of *m*/*z* 559.2 (−30 Da) is shown in Figure 8B. The strong peak at *m*/*z* 272.2 is unmodified y_2, while the peak at *m*/*z* 242.1 is $y_2 - 30$ and the peak at *m*/*z* 224.1 is $y_2 - 30 - 18$. The presence of y_2 indicates the two Asp residues contributed to the −30 Da, while the presence of $y_2 - 30$ and $y_2 - 30 - H_2O$ indicates the C-terminal carboxyl group also contributed to the −30 Da species. The peak 165.1 is 59 Da lower than *m*/*z* 224.1, and is due to the cleavage of guanidino group from $y_2 - 30 - H_2O$. The peak at 474.2 is y_4, which indicates the loss of 30 Da from the N-terminal Asp. The peak at *m*/*z* 444.1 is the $y_4 - 30$ ion. The oxidative decarboxylation of the two Asp residues is also confirmed by tandem mass spectrum of negative electrospray signals of the −30 Da product at *m*/*z* 557 (not shown), which gave rise to fragment ions b_2 at *m*/*z* 200.7, $b_2 - 30$ at *m*/*z* 170.9, b_3 at *m*/*z* 315.9, $b_3 - 30$ at 285.9, and y_2 at *m*/*z* 270.1.

Oxidation products with −30 Da mass change are also found in the radiolysis of many other Asp-contained peptides, including DRGDS, Ac-DRGDS, ADSDGK, and KQAGDV, as well as aspartic acid derivative N-acetylaspartic amide. Therefore, the oxidative decarboxylation leading to 30 Da mass reduction is characteristic for aspartic acid oxidation. The oxidative decarboxylation of Asp is expected to take place similarly to that of Glu. The kinetics of decarboxylation of Asp was examined by radiolysis of a mixture containing 30 μM Asp-NH_2 and 10 μM Glu-NH_2. The mass spectra

of the irradiated samples showed an intense −30 Da signal for Glu-NH_2 but a much weaker −30 Da signal for Asp-NH_2. This indicates that Glu is more reactive than Asp with respect to oxidative decarboxylation.

CONCLUSIONS

These data indicate that oxidative decarboxylation of acidic residues provides a molecular signature of solvent accessibility for these residues with a resulting mass loss of −30 Da for the involved peptide segments. Both Asp and Glu are susceptible to radiolytic oxidization by γ-rays or synchrotron X-rays. Reaction of Asp and Glu with hydroxyl radical under aerobic conditions results in the loss of the carboxyl group and generates an aldehyde group at the carbon next to the original carboxyl group for internal side chain oxidation. The reactivity of Glu is ∼20 times less than Phe, but ∼75% that of Pro, and higher than that for Asp. The oxidative decarboxylation also takes place at unmodified C-terminal residues and gives rise to a carbonyl group at α-carbon of the C-terminal residue. Oxidative decarboxylation leads to a primary product with characteristic mass reduction of 30 Da and minor products with mass additions of 14 and 16 Da.

An advantage of the peculiarity of oxidation products of particular side chains (as also seen for Arg oxidation) is that they represent a fingerprint for specific oxidation at that site, moderating the need for tandem MS identification of the probe residues in some cases. Although the reactivity of acidic side chains is less than for many of the amino acids that we have used as probes in the past, footprinting experiments depend on a change in reactivity at a particular site.[11,18,23,46] Reactivity depends on both intrinsic chemical reactivity and solvent accessibility. It must be pointed out that it is the solvent accessibility of the relevant reactive atoms that must be considered in order to accurately predict potential oxidation sites. Thus, although a charged moiety of a side chain may be solvent accessible, it is hydrogen abstraction from the methylene group adjacent to the COOH or the δ-carbon of Arg that must be solvent accessible and oxidized in order for the subsequent elimination reactions to occur. Despite the relatively low intrinsic reactivity of charged residues compared to, for example, aromatic residues, they are often highly solvent accessible. If they become extensively buried in an interface, they will experience a significant change in reactivity ideal for analysis by footprinting. Thus, we expect acidic side chains to be valuable probes for footprinting experiments, especially for examining protein−protein interactions.

(46) Galas, D. J.; Schmitz, A. *Nucleic Acids Res.* **1978**, *5* (9), 3157−70.

ACKNOWLEDGMENT

This research is supported in part by The Biomedical Technology Centers Program of the National Institute for Biomedical Imaging and Bioengineering under P41-EB-01979, the Innovative Molecular Analysis Technologies Program of the National Cancer Institute under R33-CA-83179, and P01-GM-66311.

Received for review December 3, 2003. Accepted January 20, 2004.

AC035422G